Bond length contraction in cobalt nanoislands on Cu(001) analyzed by surface x-ray diffraction

O. Mironets,[1] H. L. Meyerheim,[1,*] C. Tusche,[1] V. S. Stepanyuk,[1] E. Soyka,[1] H. Hong,[2] P. Zschack,[2] N. Jeutter,[3] R. Felici,[3] and J. Kirschner[1]

[1]*Max-Planck-Institut für Mikrostrukturphysik, Weinberg 2, D-06120 Halle, Germany*

[2]*APS Argonne National Laboratory, Argonne, Illinois 60439, USA*

[3]*ESRF, BP 220, F-38043 Grenoble, France*

(Received 16 August 2008; published 9 January 2009)

We present a combined surface x-ray diffraction (SXRD) and theoretical analysis of the geometric structure of nanometer sized Co islands deposited on Cu(001) at 170 K. Two-dimensional nanoislands consisting of only 20–40 atoms are characterized by a 4%–8% contraction of the interatomic distances as compared to the bulk (2.51 Å). This strongly exceeds "usual" lattice relaxations normally seen for surfaces. The SXRD analysis is based on the analysis of the registry of the Co adatoms relative to the (1×1) surface unit cell of the Cu(001) substrate crystal. Static displacements of the Co atoms of 0.18 Å (root mean square) out of the equilibrium hollow sites are observed which are in agreement with predictions based on molecular-dynamics calculations.

DOI: 10.1103/PhysRevB.79.035406 PACS number(s): 68.03.Hj, 61.05.cp, 68.43.Bc, 68.43.Fg

I. INTRODUCTION

Despite intense continuous interest on the preparation and characterization of the properties of nanosized objects, the knowledge of the geometric structure of these objects on a quantitative basis is surprisingly scarce. In general, it is well known that in low-dimensional systems interatomic distances are shorter than in their bulk analogs. Prominent examples are surface layer relaxations of the topmost layers in metallic systems.[1,2] The relaxations are attributed to the reduced coordination of the surface atoms[3] as well as to the smoothing of the charge density as suggested by Smoluchowski[4] in 1941. However, crystal surfaces still represent large systems as compared with nanosized objects such as (three-dimensional) clusters and (two-dimensional) islands, consisting of a few thousands down to only a few tens of atoms.

In this context it becomes also evident why quantitative structure data are difficult to retrieve. First of all due to their small size, conventional structure analysis techniques using electrons, x-rays, or ions in general involve an averaging over an ensemble of samples. Using nanoarea coherent electron-beam diffraction Huang *et al.*[5] investigated a single Au nanocrystal ($\varnothing\approx4$ nm) consisting of about 1000 atoms. While this approach is applicable for typical "large-scale" nanocrystals, still giving rise to a well-defined diffraction pattern, it might be less suitable for considerably smaller ones ($\varnothing\leq1$ nm) and in the case of two-dimensional objects because of the finite-size broadening of the reflection spots. On the other hand, scanning tunneling microscopy (STM), which both allows selection of a single object and—as a direct space method—avoids finite-size broadening effects, suffers from the limited *lateral* resolution necessary to unambiguously analyze atomic relaxations in the 0.05 Å range. Finally, extended x-ray absorption fine structure (EXAFS), probing the short-range order, seems not easily applicable since EXAFS probes all interatomic correlations, which in the case of a wide and probably non-Gaussian distribution of interatomic distances might lead to ambiguous results.

In our surface x-ray diffraction (SXRD) study of the structure of two-dimensional approximately 1 nm sized Co islands on Cu(001), we have followed a different approach which is based on the analysis of the registry of the nanoislands with the underlying substrate lattice. Despite the fact that the island structure does not give rise to a diffraction pattern of its own, it is long-range ordered with respect to the substrate lattice. Therefore, the Co atoms *do* contribute to the (1×1) reflections of the Cu(001) substrate, and their positions are retrievable in principle. However, the direct analysis of the adatom positions is not possible. First of all, this is because of the limited number of reflections and the large number of the atoms in an island (≈40). Second, depending on the island size and shape, the internal structure of each island slightly varies from each other, while the x-ray beam averages over a macroscopic surface area covered by about 10^{13} islands. In effect, this leads to an additional variation in atomic Co sites.

For this reason, our analysis is based on a statistical approach. Here, the well-known equilibrium adlayer structure with Co atoms residing in hollow sites of the Cu-surface is assumed.[6] It corresponds to a lateral distance of 2.56 Å between the Co atoms. Any shortening of the interatomic distances must lead to a shift of Co atoms out of the hollow sites, which is taken into account by a *static* distribution of Co-positions around the hollow site. In the simplest way the disorder can be represented by a Debye-Waller-type damping of the scattered intensity. In this approach, the number of fitting parameters to describe the disorder reduces to one, namely, the width of the Gaussian distribution function. In this context SXRD strongly benefits from the applicability of the single-scattering theory allowing a straightforward refinement and interpretation of the results, some of which have been published previously.[7]

In this paper we present a more detailed analysis of the static disorder (isotropic and anisotropic) of the Co adatoms and show that the width of the Gaussian distribution of the Co atoms out of the Cu(001) hollow site positions as derived from the SXRD data [root mean square (rms) ≈0.18 Å] is in excellent agreement with molecular-dynamics (MD) calculations. This represents a direct proof for large contractions of the interatomic distances within the two-dimensional nanoislands.

 ©2009 The American Physical Society

The paper is organized as follows. Section II outlines the experimental part including the sample preparation and STM characterization. Section III presents the results of the molecular-dynamics calculations, which are compared with the results of the SXRD intensity analysis in Sec. IV. It also critically discusses the accuracy of the SXRD results in the context of parameter correlations and the validity of the assumption of a Gaussian distribution function. Section V summarizes the results.

II. EXPERIMENT

We have chosen Co/Cu(001) since it represents a prototype system for the study of nucleation, growth, and structure of a heteroepitaxial system.[6,8–14]

The experiments were carried out *in situ* in different ultrahigh-vacuum (UHV) systems for the STM and the SXRD experiments. Two sets of SXRD experiments were carried out at different storage rings, namely, at the Advanced Photon Source (APS) in Argonne (USA) and at the European Synchrotron Radiation Facility (ESRF) in Grenoble (France) using standard UHV diffractometer setups.

Co was deposited on the clean Cu(001) surface by electron-beam evaporation from a high-purity rod. In order to grow Co islands without intermixing, the substrate temperature was kept at $T=170$ K. Experimental studies have shown that intermixing starts at about 320 K,[13] showing up in a bimodal island size distribution.[10] Absence of intermixing is concluded from STM images, revealing a Poisson-type island size distribution according to standard nucleation theory.[15]

The precise calibration of the Co coverage is a prerequisite for obtaining meaningful results in the quantitative SXRD analysis. To this end the deposition rate was calibrated by following the intensity oscillations of the (1 0 0.1) reflection versus time. This is close to the antiphase condition (100) according to the primitive setting of the surface (1×1) unit cell.[16] The calibration was carried out at 300 K to ensure layer-by-layer growth as evidenced by the periodic intensity oscillations as shown in Fig. 1. Maxima and minima correspond to complete and half filled layers, respectively. Note, that the first maximum is almost completely suppressed due to double layer growth of Co up to a coverage of two monolayers (ML).[9,17] The coverage 1 ML is defined as one adatom per substrate atom corresponding to 1.54×10^{15} atoms/cm^2.

The deposition rate is $F=0.32\pm0.02$ ML/min, which was kept constant for all experiments. Using this calibration, low coverage samples ($\theta_{Co}=0.1-0.4$ ML) were prepared for the SXRD study. Several examples are shown in Fig. 1 by the data points, which represent the time dependence of the intensity during Co deposition at 170 K. For better comparison, the intensity scattered by the uncovered Cu(001) surface is normalized to 1.0. The intensity drop during deposition is very well reproducible indicating a constant rate and allowing the deposition of an accurately calibrated amount of Co; some of them are labeled on the basis of the elapsed deposition time. After switching off the source, no further intensity change is observed.

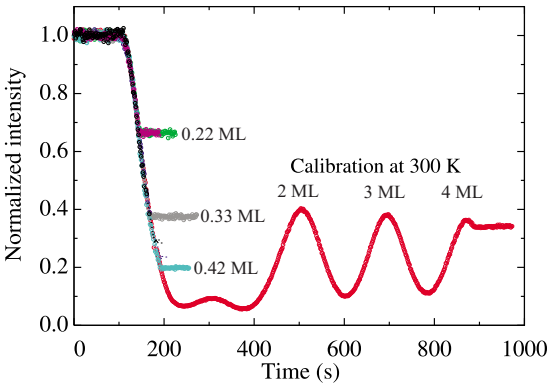

FIG. 1. (Color online) Intensity of the (1 0 0.1) reflection versus time. The calibration experiment extending to 4 ML was carried out at 300 K. The intensity of the uncovered sample is normalized to 1.0, and the deposition starts at $t\approx100$. Intensity vs time measurements for several low coverage depositions at 170 K are shown by the colored data points running horizontal after the source has been switched off.

It should be noted that the coverage was simultaneously determined by measuring the total charge collected from the ions of the partially ionized metal vapor using the flux monitor of the evaporation source (see, e.g., Ref. 18 for more details) as well as by the intensity drop at the beginning of the evaporation. We estimate an error bar of $\Delta\theta=5-10$ % corresponding to about 0.01–0.04 ML.

The deposited films were characterized by STM. The STM topography images were obtained in the constant-current mode using a W tip. Typical tunneling parameters were $I=2.0$ to 3.0 nA for the current, and 0.5 to 2.0 V for the bias voltage. Representative examples of the STM images of Co nanoislands on Cu(001) are shown in Fig. 2.

Images correspond to submonolayer coverage as indicated. Co atoms form nanoislands with an in-plane diameter of about 1 nm (bright). For the samples in the regime up to $\approx$0.5 ML Co coverage, most of the islands are of monolayer height; only a few of them (less than 1% of the total area) are bilayer islands.

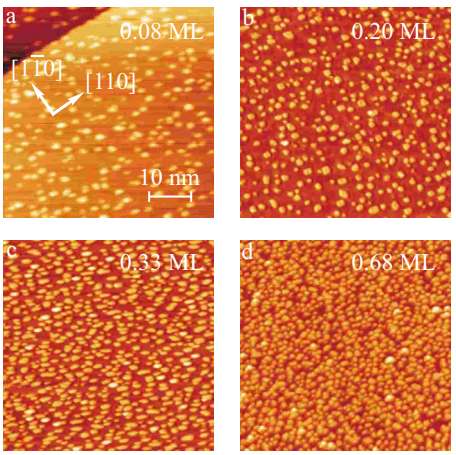

FIG. 2. (Color online) 50×50 nm^2 STM images of different Co coverage on Cu(001).

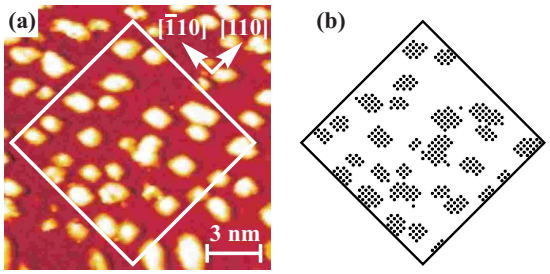

FIG. 3. (Color online) (a) 15×15 nm^2 STM image of 0.28 ML Co on Cu(001). (b) Positions of the Co atoms (black dots) within the frame in (a) used as unrelaxed starting model for the MD calculations.

III. MOLECULAR-DYNAMICS CALCULATIONS

In this section the predictions of the MD calculations with regard to the Co-island structure and their implications for the SXRD measurements are discussed.

The MD method[19] is based on a second-moment approximation of the tight-binding scheme (TB-SMA) (Ref. 20) where the many-body potentials are used for the description of the attractive energy. The MD calculations for Co-nanoislands on Cu(001) have predicted a large contraction of the interatomic distances for the simple case of square $N\times N$ Co nanoislands.[11] Therefore, for the quantification of the lattice mismatch it is not appropriate to use the conventional macroscopic lattice mismatch (M) defined as: $M=(a_{\mathrm{Cu}}-a_{\mathrm{Co}})/a_{\mathrm{Cu}}$, where $a_{\mathrm{Cu}}=2.556$ Å and $a_{\mathrm{Co}}=2.506$ Å are the bulk interatomic distances of fcc-Cu and fcc-Co, respectively. Instead Stepanyuk *et al.*[12] proposed to use the parameter m defined as $m=(r_0-r_b)/r_0$, with r_b and r_0 being the *average* interatomic distance in the Co islands and the atomic distance in Cu bulk, respectively. This is commonly referred to as the "mesoscopic misfit."

Since the $N\times N$ square islands represent idealized systems, for the comparison with experiments an island morphology closer to that observed in STM images was used in the MD calculations. The procedure is outlined on the basis of Fig. 3.

Co islands (bright areas) cover 28% of the Cu(001) surface (darker areas). The islands are in the 1–2 nm size range and consist of 10–20 atoms, in some cases up to 40 atoms. The unrelaxed Co-positions were derived by superimposing a square 10×10 nm^2 area (white frame) with a square mesh of 2.56×2.56 Å^2 in size corresponding to the Cu-(1×1) unit cell on the STM image. In this way the bright areas in the image were converted to discrete points representing the unrelaxed Co-positions shown in Fig. 3(b) as black dots. The system for the calculation takes into account, 431 Co atoms and the first nine Cu layers each containing 1521 atoms. Using this model system the MD calculation was carried out, whose most important results are summarized in Figs. 4 and 5.

The fully *relaxed* positions of the Co atoms within the (1×1) unit cell are shown as open circles in Fig. 4(a). The individual positions of all Co atoms are projected into one (1×1) unit cell, where the center position corresponds to the hollow site. It can be seen that a large fraction of Co atoms does not reside in the hollow sites but is shifted by up to 0.3 Å. The analysis of the width of the distribution is the fundamental concept of our analysis of the mesoscopic misfit.

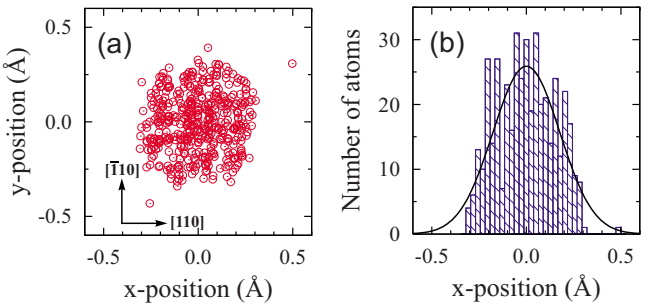

FIG. 4. (Color online) MD calculation for 0.28 ML Co/Cu(001). (a) Positions of Co atoms within the Cu(001) surface unit cell. (b) Distribution projected to the [110] direction (x axis) together with Gaussian fit (solid line).

Figure 4(b) shows the distribution of the Co-positions in a projection along the [1̄10] direction. The solid line represents a Gaussian fit with a half-width at half maximum (HWHM) of 0.069 lattice units equivalent to an rms displacement amplitude of $\sqrt{\langle u^2\rangle}=0.18$ Å. Thus, the static displacement is considerably larger than the thermal vibration amplitude. For instance, at 170 K the rms vibration amplitude is calculated to be of the order of 0.05 Å,[21] roughly a factor 4 smaller.

The MD calculation also provides a detailed picture of the distribution of the interatomic distances, which is sketched in Fig. 5. The interatomic distances are significantly smaller than the bulk value of Co (2.51 Å) and Cu (2.56 Å), represented by the vertical lines. The distribution extends over a wide range of about 0.2 Å with two maxima at 2.40 and 2.46 Å, the average being 2.44 Å corresponding to a mesoscopic misfit of $m=4.65\%$.

IV. SURFACE X-RAY DIFFRACTION

A. Analysis of the mesoscopic misfit (isotropic disorder)

SXRD is based on single-scattering theory, greatly facilitating the structure determination. The analysis of the intensity distribution along the crystal truncation rods (CTRs) is

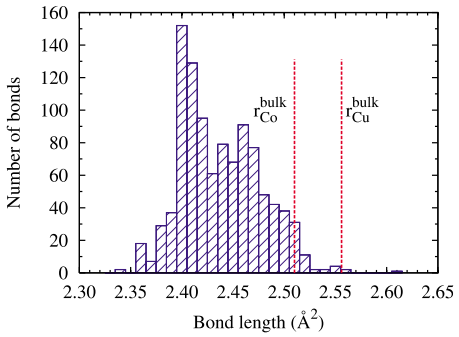

FIG. 5. (Color online) MD calculated distribution of interatomic Co-Co distances. Bulk interatomic distances for Cu and Co are indicated by the vertical lines.

the basis of the determination of the registry between the Cu(001) substrate crystal and the adsorbate atoms.

CTRs arise due to the truncation of the crystal leading to a rod of intensity along the surface normal.[22] Therefore, the reflection index ℓ becomes a continuous parameter. The total scattered structure factor (F_{tot}) is given by the interference between the structure factor of the semi-infinite substrate (F_{sub}) and the contribution of the adsorbate atoms, $|F_{\mathrm{tot}}| = |F_{\mathrm{sub}} + F_{\mathrm{Ad}} \exp[i\phi]|$, where the phase factor $\phi = 2\pi[hx + ky + \ell z]$ takes into account the registry of the Co atoms. Here the Co atoms occupy the position $(x = 1/2, y = 1/2, z)$, corresponding to the hollow site within the (1×1) surface unit cell. If absorption is neglected, the substrate structure factor (F_{sub}) is given by $F_{\mathrm{sub}} = f_{\mathrm{Cu}}/\{1 - \exp[-i\pi(h+k+\ell)]\}$, where f_{Cu} represents the atomic scattering factor for Cu.[21]

At the antiphase condition given by $h+k+\ell = 2n+1$ (n=integer) the total scattered intensity of the substrate is proportional to 0.25 ML: $I(hk\ell) \propto |F_{\mathrm{sub}}|^2 = f_{\mathrm{Cu}}^2/4$. It is the suppression of the substrate scattering contribution at positions in reciprocal space off the bulk Bragg-positions ($h+k+\ell = 2n$), which makes the analysis "surface sensitive."

The adsorbate contribution (F_{ad}) can be written as a product of three terms, namely, the relative adsorbate coverage (θ_{Co}), the atomic scattering amplitude of Co (f_{Co}) and the displacement factor $T(\vec{q})$: $F_{\mathrm{ad}} = \theta_{\mathrm{Co}} \cdot f_{\mathrm{Co}} \cdot T(\vec{q})$, the latter representing the Fourier transform of the probability density function, pdf($\vec{r}$), describing the displacement field (thermal and static) of the atoms out of the equilibrium position (for details see Refs. 23 and 24). In many cases pdf($\vec{r}$) can be approximated reasonably well by a spherically symmetric Gaussian-distribution function,

$$\mathrm{pdf}(\vec{r}) = \mathrm{pdf}(r) = \frac{1}{(2\pi\langle u^2\rangle)^{3/2}} \exp[-r^2/2\langle u^2\rangle], \qquad (1)$$

leading to a simple analytic function for $T(q)$ as follows: $T(q) = \exp[-B \cdot q^2/4]$. This corresponds to the well-known Debye-Waller damping factor containing the rms displacement amplitude $\sqrt{\langle u^2\rangle}$, which enters the Debye parameter (B) by $B = 8\pi\langle u^2\rangle$.

Using $q = 0.39$ Å^{-1} for the (100) reflection and $\sqrt{\langle u^2\rangle} = 0.18$ Å ($B = 2.56$ Å^2) from the MD calculations, one obtains $T(q = 0.39\ \text{Å}^{-1}) = 0.90$, i.e., the static displacement reduces the total structure factor amplitude of the adlayer by about 10% relative to that of the ordered structure. This estimate shows that the measured intensities must be collected with high accuracy in order to derive meaningful results. In addition, correlations with other parameters such as relaxations and thermal disorder of the Cu-substrate atoms need to be considered (see below). First we discuss the experimental results.

Integrated x-ray intensities (I_{obs}) were collected by rotating the sample about the surface normal under grazing incidence of the incoming beam (wavelength $\lambda = 0.62$ Å). Structure factor amplitudes, $|F_{\mathrm{obs}}| \propto \sqrt{I_{\mathrm{obs}}}$, were derived by correcting the integrated intensities for apparative factors.[25] In total 11 data sets were collected at 170 K following eight independent preparations. Each data set consists of about 300–350 reflections along 18 CTRs reducing to about 150–180 independent reflections along 9 CTRs by symmetry equivalence. Due to the high beam intensity the total standard deviation (σ_F) for $|F_{\mathrm{obs}}|$ is dominated by the reproducibility of symmetry equivalent reflection intensities,[26] which lies between 4% and 9%.

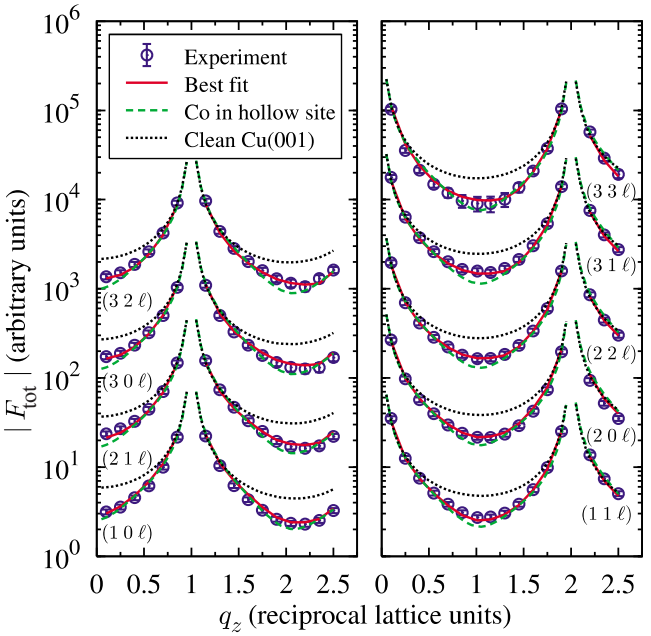

FIG. 6. (Color online) Measured (symbols) and calculated (lines) structure factor amplitudes for 0.30 ML Co/Cu(001). Solid lines represent the best fit; dashed and dotted lines correspond to models with Co in hollow sites only and the clean Cu(001), respectively. Curves are shifted for clarity.

As an example, Fig. 6 shows the CTRs for 0.3 ML Co. Symbols and error bars represent the measured $|F_{\mathrm{obs}}|$ and σ_F, respectively. CTRs were measured in steps of $\Delta\ell = 0.15$ reciprocal lattice units (rlus) (1 rlu $= c^* = 1/c = 1/3.616$ Å $= 0.277$ Å^{-1}) up to the maximum momentum transfer of $q_z = 2.5$ rlu. The distribution of $|F_{\mathrm{obs}}|$ along q_z exhibits the typical U shape when plotted on a logarithmic scale; their (omitted) maxima at $\ell = 0, 1, 2$ correspond to the positions of the bulk Bragg reflections.

Lines in Fig. 6 represent different calculated CTRs as follows. (i) The black dotted line is related to the uncovered bulk truncated Cu(001) crystal. (ii) The dashed (green) line is obtained by assuming a fraction of 0.3 ML of Co atoms located in hollow sites and thermal disorder only, which is of the order of $B = 0.34$ Å^2 at 170 K. Although the intensity reduction due to the Co adsorption is reproduced (see also Fig. 1), detailed inspection reveals deviations between calculated and observed CTRs. The differences are most pronounced close to the antiphase conditions ($\exp[i\phi] = -1$) and they increase with increasing magnitude of the scattering vector. This is a direct indication for a Debye-Waller-type damping of the adlayer scattering amplitude. (iii) In the best-fit model shown by full (red) lines the Debye parameter of the Co layer B_{Co} is 2.6 ± 0.4 Å^2. It corresponds to the rms displacement amplitude of 0.182 ± 0.015 Å in excellent agreement with the MD calculation. This is the most important result of our study.

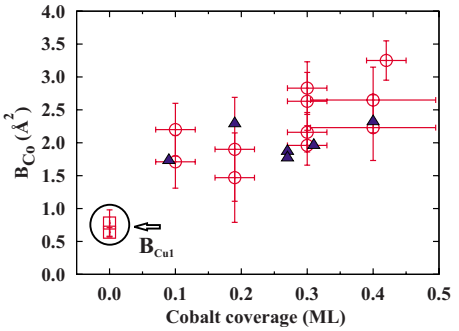

FIG. 7. (Color online) Debye parameters of Co (open circles) versus Co coverage. Simulated data based on MD calculations are represented by triangles. The Debye parameters for first layer Cu atoms for uncovered Cu(001) are shown as squares at zero coverage (see label B_{Cu1}).

Figure 7 provides an overview over the results. The open symbols represent the refined (isotropic) Debye parameters versus Co coverage. Error bars of ± 0.50 Å^2 are estimated on the basis of the reproducibility of independent experiments and on the correlations with other parameters as discussed below. It can be seen that for all independent experiments B factors in the range between 1.8 and 3.2 Å^2 are derived; the average being 2.5 Å^2.

As outlined in Sec. II, several STM images recorded at different coverages were used as starting configurations in MD calculations. Using the atomic coordinates derived from theory, we used them to calculate the total structure factor amplitudes ($|F_{tot}|$). In turn, using these theoretical structure factor amplitudes, the data analysis was carried out in the same way as with the "true" experimental ones. The result for B_{Co} is represented by the triangles in Fig. 7. The agreement with the experimental data is quite convincing; some scatter in B_{Co} is attributed to correlation effects with other parameters and to differences in the island sizes and shapes. The scatter in the theoretically derived values is about same as the estimated errors for the experimentally derived B factors.

In order to achieve high quality fits it is not sufficient to take account of the adlayer disorder only but it also requires the consideration of several further parameters. Apart from the B factor of Co (B_{Co}), also the Debye parameters of three top Cu layers ($B_{Cui}, i=1,2,3$) were refined. Deeper layers were treated as bulklike (B_{bulk}), which was also refined. In addition to the Debye parameters, z positions of up to four top Cu layers and that of the Co layer were allowed to vary. The interlayer spacing between deeper layers was set to the bulk Cu value $d_{Cu}=1.81$ Å. The Co layer occupancy θ_{Co} was fixed at the calibrated values as outlined above (see Fig. 1).

Excluding an overall scale factor this adds up to in total up to $P=8$ adjustable parameters, which in comparison with the total number of independent reflections ($N=150-180$) ensures a reasonable overdetermination of the fit problem. It should be emphasized that the correlations between the parameters can play a more important role than the N/P ratio, especially in the context of the analysis of "soft" parameters such as the Debye parameters (see below).

We briefly summarize the results for the B factors and the structural parameters for the 0.3 ML sample; a complete overview is provided by Table I. The Debye parameter of the top two Cu layers are $B_{Cu1}=0.59\pm0.05$ Å^2 and $B_{Cu2}=0.33\pm0.02$ Å^2. The bulk Debye parameter is 0.26 ± 0.02 Å^2, which is close to the calculated thermal Debye parameter at 170 K (0.34 Å^2).[21] The APS derived values for the Debye parameters of the Cu layers are generally somewhat smaller ($\approx 0.3-0.5$ Å^2) than those derived from the measurements at the ESRF. We tentatively attribute this to differences in the details of the data (e.g., standard deviations and number of reflections). It should be noted that the error bars listed in Table I are derived from the fitting procedure based on the variance-covariance matrix, while the total uncertainty as estimated from the reproducibility of independent measurements lies in the 0.5 Å^2 range as will be discussed below in Sec. IV C.

For the Co adsorption height (d_{Co-Cu}) we find 1.78 ± 0.08 Å corresponding to a 1.5% contraction relative to the bulk Cu spacing. The first Cu interlayer distance is also contracted by 1.5%, but deeper layers are not relaxed within the experimental uncertainty.

Our findings are in good agreement with previous studies. For instance, the low-energy electron diffraction (LEED) analysis of Cerda *et al.*[6] determined a Co-adsorption height of $d_{Co-Cu}=1.76\pm0.03$ Å in comparison with the average value 1.79 ± 0.03 Å of this study. Similarly $d_{12}=1.78\pm0.03$ Å from Ref. 6 is identical with our (average) value for d_{12}.

Without exception, high-quality fits were obtained. The fit quality is quantified by several agreement criteria, namely, the goodness of fit (GOF) and the unweighted residual (R_u).[29] The GOF values for 11 data sets lie in the range between 0.9–1.6, the unweighted residua R_u are between 4% and 6%. These numbers can be considered as excellent for SXRD data analysis.

In two additional experiments we have also studied the structure of *uncovered* Cu(001) for comparison. A more detailed discussion of these measurements is presented in Ref. 30. Their aim was to "calibrate" our experimental accuracy by comparison with previous studies investigating the comparatively small thermal disorder of the top layer atoms of the uncovered Cu(001) surface.[27,28] The comparison is very encouraging: the SXRD analysis allows a precise determination of the enhancement of surface thermal vibrations. The results are listed in the upper part of Table I.

In contrast to the very large values for B_{Co} of the Co-covered samples, the Debye parameters B_{Cu} for the topmost Cu layers of the Cu(001) substrate are rather low: $B_{Cu(1)}=0.64\pm0.07$ Å^2 and 0.79 ± 0.20 Å^2 (two independent measurements at APS and ESRF). These values are about 70% larger than in the bulk at 170 K as expected for the thermal vibration amplitudes for surface atoms. They are in good agreement with previous studies.[27,28] Debye parameters of deeper layers rapidly approach the bulk value within a few layers (see Ref. 30).

B. Anisotropic displacements

So far, it was assumed that the displacement of the Co atoms is isotropic; i.e., the description of the static disorder

TABLE I. SXRD-derived structure parameters for clean and Co-covered samples. † and ‡ denote APS and ESRF data, respectively.

	Debye parameters (Å^2)					Interlayer distances (Å)				
	B_{Co}	B_{Cu1}	B_{Cu2}	B_{Cu3}	B_{bulk}	d_{Co-Cu}	d_{12}	d_{23}	d_{34}	d_{45}
		Clean Cu(001):								
†		0.64(9)	0.23(7)	0.17(5)	0.17(5)		1.79(4)	1.82(4)	1.81(4)	1.81(3)
‡		0.79(20)	0.54(9)	0.42(5)	0.34(4)		1.78(3)	1.81(3)	1.81(3)	1.81(2)
Ref. 27		0.93								
Ref. 28		0.47								
		0.10 ML Co/Cu(001):								
‡	1.71(39)	1.12(17)	0.84(7)	0.74(3)	0.68(3)	1.76(9)	1.77(4)	1.81(3)	1.80(1)	Bulk
‡	2.20(44)	1.16(22)	0.69(6)	0.52(3)	0.45(3)	1.77(9)	1.79(3)	1.81(3)	1.80(2)	Bulk
		0.19 ML Co/Cu(001):								
†	1.47(68)	0.43(4)	0.28(2)	0.22(2)	0.22(2)	1.81(9)	1.78(3)	1.82(3)	1.81(3)	1.81(1)
†	1.90(79)	0.45(5)	0.26(2)	0.21(2)	0.21(2)	1.76(10)	1.79(4)	1.82(4)	1.81(3)	1.81(2)
		0.30 ML Co/Cu(001):								
†	2.90(44)	0.59(5)	0.33(2)	0.26(2)	0.26(2)	1.78(8)	1.78(4)	1.81(4)	1.81(3)	1.81(2)
†	2.83(32)	0.78(4)	0.43(2)	0.37(1)	0.37(1)	1.86(6)	1.77(3)	1.81(3)	1.81(2)	1.81(1)
‡	1.96(32)	1.16(17)	0.99(6)	0.91(3)	0.89(2)	1.79(7)	1.78(3)	1.81(3)	1.80(1)	Bulk
‡	2.16(35)	1.15(14)	0.84(7)	0.75(3)	0.71(3)	1.78(9)	1.79(4)	1.81(3)	1.80(2)	Bulk
		0.40 ML Co/Cu(001):								
†	2.65(42)	0.63(7)	0.28(2)	0.18(2)	0.18(2)	1.77(10)	1.79(4)	1.82(4)	1.81(4)	1.80(2)
†	2.23(33)	0.60(7)	0.20(2)	0.13(2)	0.13(2)	1.81(9)	1.80(5)	1.82(4)	1.81(3)	1.81(2)
		0.42 ML Co/Cu(001):								
‡	3.25(35)	1.36(15)	0.85(7)	0.74(4)	0.70(4)	1.78(9)	1.79(3)	1.80(3)	1.81(2)	Bulk
		1 ML Co/Cu(001)								
		Ref. 6				1.76(3)	1.78(3)			

was based on a harmonic isotropic model, in which the probability density function $[\mathrm{pdf}(\vec{r})]$ is represented by a spherically symmetric Gaussian function as given by Eq. (1). Although the results of the analysis are generally quite convincing the assumption of an isotropic displacement distribution might be challenged by the MD calculations using the idealized square $N\times N$ islands.[11] In these it was shown that the vertical displacements of the Co-island atoms and those of the underlying Cu atoms are considerably smaller than the in-plane ones. Quantitatively, the maximum vertical height difference within a 6×6 island was calculated to be 0.072 Å, about the magnitude of thermal vibrations. Similar values were also found for the modification of the z positions for the Cu atoms below the Co island.

In order to investigate this prediction in more detail we went one step further by allowing for an anisotropy of the displacements. Taking into account the point-group symmetry of the average structure (plane group $p4mm$) the anisotropic pdf can be written as

$$\mathrm{pdf}(\vec{r}) = \frac{1}{(2\pi)^{3/2}\sqrt{\langle u_{\parallel}^2\rangle^2\langle u_{\perp}^2\rangle}}\exp\left[-\frac{1}{2}\left(\frac{x_1^2+x_2^2}{\langle u_{\parallel}^2\rangle}+\frac{x_3^2}{\langle u_{\perp}^2\rangle}\right)\right] \tag{2}$$

where subscripts $(\parallel,1)$ and $(\perp,3)$ represent the in-plane and out-of-plane directions, respectively. Note that the in-plane displacement amplitudes along the x and y axes are identical $(\langle u_{\parallel}^2\rangle=\langle u_{11}^2\rangle=\langle u_{22}^2\rangle)$ and that the axes of the pdf are parallel to the lattice axes making the off-diagonal elements of the displacement tensor to vanish.[24]

The MD calculations yield the atomic coordinates, from which the total structure factor amplitudes were calculated, which in turn were analyzed in the same way as the experimental data. Figure 8(a) shows the GOF topography versus the in-plane $(\langle u_{\parallel}^2\rangle)$ and the out-of-plane $(\langle u_{\perp}^2\rangle)$ mean-square displacement amplitude. The minimum of the GOF (cross) is found for $\langle u_{\parallel}^2\rangle=0.035$ Å^2 and $\langle u_{\perp}^2\rangle=0.003$ Å^2, quantitatively reproducing the MD predicted anisotropy of the dis-

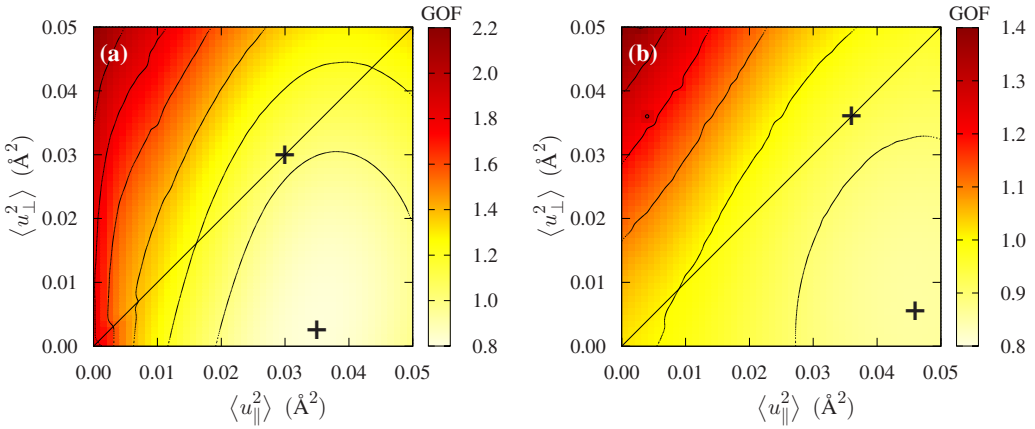

FIG. 8. (Color online) GOF topography for anisotropic displacements in 0.4 ML Co: (a) simulation based on MD calculations and (b) experiment. Crosses on the diagonal represent GOF minima for the isotropic model and crosses on the lower right correspond to absolute GOF minima including anisotropic displacements.

placements. For comparison, the diagonal line represents the condition $\langle u_\perp^2 \rangle = \langle u_\parallel^2 \rangle$, on which the cross represents the best fit at $\langle u^2 \rangle \approx 0.030$ Å^2. Note, however that the dependence of GOF on $\langle u_\perp^2 \rangle$ is rather shallow. The difference between the GOF values for the two models is below 10%. This can be attributed to the limited sampling of the reciprocal space along q_z. While the lateral momentum transfer extends up to $q_{x,y} = 1.74$ Å^{-1} in the case of the (42ℓ) rod, the maximum perpendicular momentum transfer is limited to $q_z = 0.69$ Å^{-1}. The limited sampling along q_z is an inherent problem in SXRD measurements mostly because of apparatus limitations and due to the strong intensity drop at high q_z as a result of the polarization and Lorentz factor.

Nevertheless, accurate intensity measurements allowed an analysis of the anisotropic displacements in several cases based on the criterion that including anisotropy improves the fit quality as measured by the GOF.

For instance, Fig. 8(b) shows the GOF contour plot for the 0.4 ML sample. Here, the GOF was improved from 0.93 in the case of the isotropic pdf (cross on the diagonal) with $\langle u^2 \rangle = 0.035$ Å^2 to GOF=0.85 in the case of anisotropic displacement distribution. We find $\langle u_\parallel^2 \rangle = 0.046$ Å^2 and $\langle u_\perp^2 \rangle = 0.006$ Å^2 (cross on the lower right) in good agreement with the MD calculations. Other parameters did not change within the standard deviations. The GOF topographies for theory and experiment are very similar with regard to the overall shape.

The SXRD experiment quantitatively confirms the predicted anisotropy of the displacements of the Co atoms. However it should be emphasized that allowing for anisotropy did not lead to an improvement of the GOF in all cases. Apart from the fundamental arguments concerning the reciprocal space sampling, we tentatively attribute this to the slightly different quality of the different data sets as well as to the importance of correlations of the displacement amplitudes with other fit parameters, which play an important role for the accuracy of the results. For an appropriate estimate of the error bars the possible influence of correlations was analyzed in detail; some of which are briefly discussed in Sec. IV C.

C. Analysis of correlations

Parameter correlations are an inherent problem in any least-squares refinement involving several variables.[31] High parameter correlations might severely affect the "precision" (standard uncertainty) of the refined parameters. In the present study the main focus lies on the determination of the Debye parameter $(B = 8\pi\langle u^2 \rangle)$ of the Co atoms; but a full description of the surface structure involves several other parameters such as the z positions and the B factors of the top two to three Cu layers and the z position of Co. Otherwise, no satisfying fit can be achieved. Correlations are derived from the variance-covariance matrix. The highest correlations were found to lie in the 0.7 range, most of them were significantly less (0.2–0.4). This is a favorable situation allowing the determination of B_{Co} with sufficient accuracy. Nevertheless we have carefully analyzed parameter correlations, two of them are illustrated in the following.

Figure 9 shows two examples. On the left (a) GOF is plotted as a function of B_{Co} and B_{Cu1}, the latter being the B factor of the top Cu layer, on the right (b) the GOF-topography is plotted as a function of B_{Co} and the z position of Co. The latter is expressed by the relative change in the Co-Cu spacing with respect to bulk Cu spacing: $(d_{(\mathrm{Co\text{-}Cu1})} - d_{(\mathrm{Cu})})/d_{(\mathrm{Cu})}$. All other parameters were allowed to vary.

In both cases a global GOF minimum (cross) is found, but the parameter correlations in the two cases are different. While there is (a) a positive correlation between the two Debye parameters, there is almost (b) no correlation between the Debye parameter and the z position of Co. Qualitatively similar results were obtained for other parameters indicating that the correlations are positive and relatively high between the B factors. Nevertheless, the GOF contour plots clearly indicate that the least-squares refinement leads to meaningful results.

At first the dependence of GOF versus B_{Cu1} is quite steep providing clear evidence that there is an enhancement of B_{Cu1} by about a factor of 2 over the calculated bulk value $(B_{\mathrm{bulk}} \approx 0.34$ Å). The elongated shape of the contour plot along B_{Co} can be attributed to the lower weight of the Co atoms in the fit procedure due to the small occupancy factor

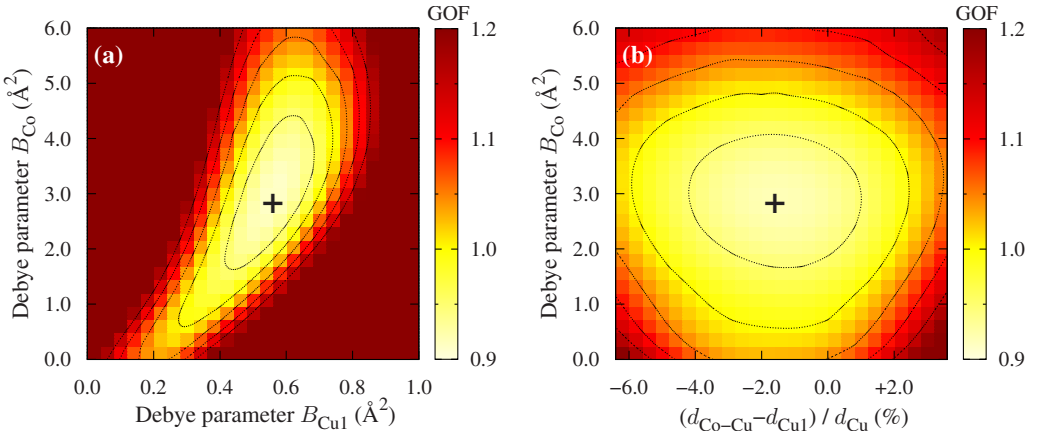

FIG. 9. (Color online) GOF contour maps showing correlations between two fits. (a) Correlation between Debye parameters B_{Co} and B_{Cu1}. (b) Correlation between B_{Co} and interlayer distance $d_{Co\text{-}Cu}$ represented by the ratio $(d_{(Co\text{-}Cu1)}-d_{(Cu)})/d_{(Cu)}$ relative to bulk Cu-interlayer spacing $d_{(Cu)}=1.8075$ Å. Crosses indicate GOF minimum.

($\theta_{Co}=0.3$ versus $\theta_{Cu1}=1.0$). Second, the GOF-topography in Fig. 9(b) shows that the vertical distance of the Co atoms (1.78 Å) to the top layer Cu atoms is smaller than the bulk Cu spacing by about 1.5%, but variation in this parameter has almost no effect on B_{Co}.

Uncertainties for the Debye parameters were estimated based on the thorough analysis of the correlations, and we find a standard deviation (1σ) of about ± 0.5 Å for B_{Co}.

D. Gaussian distribution

The study of the mesoscopic misfit presented thus far has assumed that the displacement field of the Co atoms out of the hollow site position can be approximated by a Gaussian-type distribution function pdf(u) (see, e.g., Fig. 4) leading to the simple Debye-Waller damping term, $T(q)$. Its major advantage is that it contains only the parameter $\langle u^2 \rangle$ as a fit parameter. Although the results derived on the basis of this model are in excellent agreement with the MD calculations, we have carried out calculations to investigate the effect of the exact MD-calculated *non-Gaussian* pdf distribution of the Co atoms has on the reflection intensities in comparison with those based on the Gaussian distribution. This provides an estimate on the degree of accuracy needed to determine a non-Gaussian-type distribution.

The procedure was as follows. Two kinds of distribution functions were considered, namely, the MD derived (pdf_{MD}) and a Gaussian approximation (pdf_G) in which the same numbers of atoms and the same HWHM were used. The distributions pdf_{MD} and pdf_G are compared in Fig. 10(a) as filled and open bars, respectively. Using otherwise identical structure parameters the structure factor amplitudes [$|F_{MD}(q)|$ and $|F_G(q)|$] were calculated and compared by plotting the ratio $R(q)=|F_{MD}(q)|/|F_G(q)|$ versus q_z as shown in Fig. 10(b). The ratio was calculated at the same positions in q space at which also the experimental data were collected. The calculations clearly prove that the Gaussian approximation is a very good one.

For 94% of data points $R(q)$ lies within the $\pm 5\%$ uncertainty level marked by the horizontal dashed lines. Only for ten data points at high q values, which are most sensitive to the details of the distribution function, is there a disagreement larger than 5%. Even under the assumption of a quite good experimental accuracy of 5% (1σ level) based in the structure factor amplitudes, the distributions cannot be distinguished using reflections in the accessible q range and the assumption of the pdf_G in the analysis is justified.

V. SUMMARY

Surface x-ray diffraction has been used to provide experimental evidence for the theoretically predicted concept of the

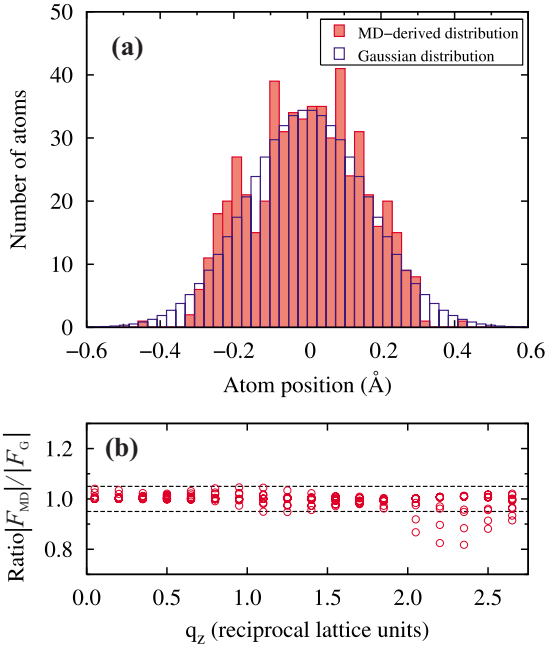

FIG. 10. (Color online) MD-derived displacement distribution out of the hollow site and Gaussian distribution (top image); ratio between the total structure factor amplitudes calculated for the MD-derived distribution and for the Gaussian distribution of atomic displacements. Dashed lines indicate the ratios in the range $\pm 5\%$.

mesoscopic misfit. It suggests strong (4%–8%) contractions of the average interatomic distances relative to the bulk in monolayer thick epitaxial metallic nanoislands consisting of several tens of atoms only. Using the Co/Cu(001) system as an example, the SXRD analysis was based on the determination of the registry of the Co adatoms relative to the Cu(001) hollow sites. The analysis of the static Gaussian disorder of the Co atoms out of the substrate hollow sites induced by the bond contraction is in excellent agreement with molecular-dynamics calculations. They derive an average interatomic distance of 2.42 Å within the Co island (bulk: 2.51 Å) leading to a half-width at half maximum of 0.18 Å (corresponding to $B_{\mathrm{Co}}=2.55$ Å^2) of the distribution function. Other structural parameters such as interlayer spacings are in good agreement with previous studies.

In addition, we have carried out detailed investigations on parameter correlations and on the validity of the assumption of a Gaussian-type disorder distribution. It could be shown that parameter correlations are generally low and therefore do not represent a problem in deriving unambiguous results for B_{Co}. Furthermore, the Gaussian distribution assumed in the intensity analysis is well justified since differences between the structure factor amplitudes for the MD calculated and the Gaussian distribution are less than 5%, i.e., below the experimental accuracy.

ACKNOWLEDGMENTS

H.L.M., C.T., and O.M. thank the ESRF and APS staff for their help and hospitality during their stay in Grenoble and Argonne. Use of the Advanced Photon Source was supported by the U.S. Department of Energy, Office of Science, Office of Basic Energy Sciences under Contract No. W-31-109-Eng-38.

*hmeyerhm@mpi-halle.mpg.de

[1] G. A. Somorjai, *Introduction to Surface Chemistry and Catalysis* (Wiley, New York, 1994).
[2] F. Jona and P. M. Marcus, in *The Structure of Surfaces II*, Springer Series in Surface Science Vol. 11, edited by J. F. van der Veen and M. A. Van Hove (Springer-Verlag, Berlin, 1988), p. 90.
[3] L. Pauling, J. Am. Chem. Soc. **69**, 542 (1947).
[4] R. Smoluchowski, Phys. Rev. **60**, 661 (1941).
[5] W. J. Huang, R. Sun, J. Tao, L. D. Menard, R. G. Nuzzo, and J. M. Zuo, Nature Mater. **7**, 308 (2008).
[6] J. R. Cerdá, P. L. de Andres, A. Cebollada, R. Miranda, E. Navas, P. Schuster, C. M. Schneider, and J. Kirschner, J. Phys.: Condens. Matter **5**, 2055 (1993).
[7] O. Mironets, H. L. Meyerheim, C. Tusche, V. S. Stepanyuk, E. Soyka, P. Zschack, H. Hong, N. Jeutter, R. Felici, and J. Kirschner, Phys. Rev. Lett. **100**, 096103 (2008).
[8] F. J. Lamelas, C. H. Lee, Hui He, W. Vavra, and Roy Clarke, Phys. Rev. B **40**, 5837 (1989).
[9] J. Fassbender, R. Allenspach, and U. Durig, Surf. Sci. **383**, L742 (1997).
[10] F. Nouvertné, U. May, M. Bamming, A. Rampe, U. Korte, G. Güntherodt, R. Pentcheva, and M. Scheffler, Phys. Rev. B **60**, 14382 (1999).
[11] V. S. Stepanyuk, D. I. Bazhanov, A. N. Baranov, W. Hergert, P. H. Dederichs, and J. Kirschner, Phys. Rev. B **62**, 15398 (2000).
[12] V. S. Stepanyuk, D. I. Bazhanov, W. Hergert, and J. Kirschner, Phys. Rev. B **63**, 153406 (2001).
[13] R. Pentcheva, K. A. Fichthorn, M. Scheffler, T. Bernhard, R. Pfandzelter, and H. Winter, Phys. Rev. Lett. **90**, 076101 (2003).
[14] S. Pick, V. S. Stepanyuk, A. L. Klavsyuk, L. Niebergall, W. Hergert, J. Kirschner, and P. Bruno, Phys. Rev. B **70**, 224419 (2004).
[15] J. A. Venables, in *The Chemical Physics of Solid Surfaces*, edited by D. A. King and D. P. Woodruff (Elsevier, Amsterdam, 1997), Vol.8; J. A. Venables, G. D. Spiller, and M. Hanbücken, Rep. Prog. Phys. **47**, 399 (1984).
[16] The primitive settings for surface diffraction correspond to the settings used in the conventional bulk x-ray diffraction by the following relations: $[100]_s=\frac{1}{2}\{[100]_b+[010]_b\}$, $[010]_s=\frac{1}{2}\{[100]_b-[010]_b\}$, $[001]_s=[001]_b$.
[17] A. K. Schmid and J. Kirschner, Ultramicroscopy **42-44**, 483 (1992).
[18] J. Kirschner, H. Engelhard, and D. Hartung, Rev. Sci. Instrum. **73**, 3853 (2002).
[19] N. A. Levanov, V. S. Stepanyuk, W. Hergert, D. I. Bazhanov, P. H. Dederichs, A. A. Katsnelson, and C. Massobrio, Phys. Rev. B **61**, 2230 (2000).
[20] V. Rosato, M. Guillope, and B. Legrand, Philos. Mag. A **59**, 321 (1989).
[21] *International Tables for X-Ray Crystallography*, edited by C. H. MacGillavry, G. D. Reick, and K. Lonsdale (Reidel, Dordrecht, 1985), Vol. 3.
[22] I. K. Robinson, Phys. Rev. B **33**, 3830 (1986).
[23] W. H. Kuhs, Acta Crystallogr. A **48**, 80 (1992).
[24] M. J. Buerger, *Kristallographie* (Walter de Gryuter, Berlin, 1977), pp. 363–367.
[25] E. Vlieg, J. Appl. Crystallogr. **30**, 532 (1997).
[26] R. Feidenhans'l, Surf. Sci. Rep. **10**, 105 (1989).
[27] D. E. Fowler and J. V. Barth, Phys. Rev. B **52**, 2117 (1995).
[28] L. Yang, T. S. Rahman, and M. S. Daw, Phys. Rev. B **44**, 13725 (1991).
[29] Unweighted residual $R_u=\Sigma||F^{\mathrm{obs}}|-|F^{\mathrm{calc}}||/\Sigma|F^{\mathrm{obs}}|$, with F^{obs} and F^{calc} as the observed and calculated structure factors, respectively. For GOF see Ref. 26.
[30] O. Mironets, H. L. Meyerheim, C. Tusche, P. Zschack, H. Hong, N. Jeutter, R. Felici, and J. Kirschner, Phys. Rev. B **78**, 153401 (2008).
[31] E. Prince, *Mathematical Techniques in Crystallography and Materials Science* (Springer, Berlin, Heidelberg, 1982).